JOC The Journal of Organic Chemistry

Subscriber access provided by University of Wollongong Library

Note

Close Amide NH···F Hydrogen Bonding Interactions in 1,8-Disubstituted Naphthalenes

Muhammad Kazim, Maxime A. Siegler, and Thomas Lectka

J. Org. Chem., **Just Accepted Manuscript** • DOI: 10.1021/acs.joc.0c00553 • Publication Date (Web): 31 Mar 2020

Downloaded from pubs.acs.org on April 4, 2020

Just Accepted

"Just Accepted" manuscripts have been peer-reviewed and accepted for publication. They are posted online prior to technical editing, formatting for publication and author proofing. The American Chemical Society provides "Just Accepted" as a service to the research community to expedite the dissemination of scientific material as soon as possible after acceptance. "Just Accepted" manuscripts appear in full in PDF format accompanied by an HTML abstract. "Just Accepted" manuscripts have been fully peer reviewed, but should not be considered the official version of record. They are citable by the Digital Object Identifier (DOI®). "Just Accepted" is an optional service offered to authors. Therefore, the "Just Accepted" Web site may not include all articles that will be published in the journal. After a manuscript is technically edited and formatted, it will be removed from the "Just Accepted" Web site and published as an ASAP article. Note that technical editing may introduce minor changes to the manuscript text and/or graphics which could affect content, and all legal disclaimers and ethical guidelines that apply to the journal pertain. ACS cannot be held responsible for errors or consequences arising from the use of information contained in these "Just Accepted" manuscripts.

is published by the American Chemical Society. 1155 Sixteenth Street N.W., Washington, DC 20036

Published by American Chemical Society. Copyright © American Chemical Society. However, no copyright claim is made to original U.S. Government works, or works produced by employees of any Commonwealth realm Crown government in the course of their duties.

Close Amide NH···F Hydrogen Bonding Interactions in 1,8-Disubstituted Naphthalenes

Muhammad Kazim, Maxime A. Siegler and Thomas Lectka*

Department of Chemistry, Johns Hopkins University, 3400 North Charles Street, Baltimore, MD, 21218.

ABSTRACT: In this note, we present a series of N-(8-fluoronaphthalen-1-yl)benzamide derivatives designed to maximize amide-NH···F hydrogen bond interactions therein. A combination of IR and NMR spectroscopy indicates a linear correlation between the high energy shift in NH stretching frequency and the electron withdrawing nature of the substituent, consistent with the trend predicted by DFT calculations. Additionally, a limiting case of hydrogen bonding is observed when the benzamide derivatives are replaced with trifluoroacetamide, causing an additional red shift of 44 cm^{-1} in the NH stretching frequency. Most importantly, ^{1}H-^{19}F coupling constants in this series are among the largest measured for amide-NH···F interactions. X-ray crystallography reveals face-to-face alignment of naphthalene rings in these derivatives resulting in part from the NH···F hydrogen bonds. This motif also dictates the formation of sheets composed of stacked naphthalene rings in the crystal structure as opposed to unfluorinated analogues wherein NH···OC hydrogen-bonding interactions force benzamide and naphthalene rings to engage in T-shaped π–π interactions instead. Additionally, the NH proton in the trifluoroacetamide derivative engages in extended H-bond interactions in its crystal structure.

The interaction of C-F bonds, especially in proteins, with proximate functional groups is a topic of lively interest and discussion.[1-6] Their importance in dictating protein structure and function is not yet fully answered, including the dilemma of whether such interactions themselves are due to propinquity, attractive interactions, or a combination thereof. Over the past several years we have investigated close interactions between C-F bonds and common organic functional groups in relatively small molecules that are often dictated by forced proximity, along with some measure of attraction and repulsion.[7-13] The case of the amide NH···F interaction is presumably one of the more interesting, due to the ubiquity of amide residues in proteins. Nevertheless, a search of the Cambridge Crystallographic Database (CCD) indicates only a few substantial interactions; most are self-evidently weak and long range. The closest such interaction we found was approximately 1.93 Å.[14] We thought it would be illustrative and useful to investigate the closest range and thus strongest model interaction we could conceive in order to achieve a fuller understanding. In this note, we employ the 1,8-disubstituted naphthalene scaffold to investigate a series of amide NH···F interactions that are by spectroscopic measures more intense than those exhibited in the available crystal structure database. Historically, these so-called "proton sponge" derivatives have often been used to investigate the nature of close H-bonding interactions.[15-20] We imagined that a series of these molecules would once again serve as excellent models for the study of amide-NH···F interactions (Figure **1**).

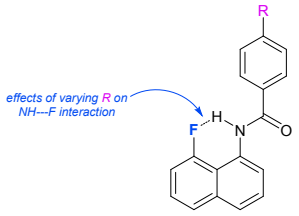

Figure 1. *The NH···F Interaction in N-(8-fluoronaphthalen-1-yl)benzamide derivatives*

Chemical intuition suggests that the *trans*-amide conformation of these *N*-(8-fluoronaphthalen-1-yl)benzamide derivatives would make the N-H proton particularly available to engage in hydrogen bonding to the neighboring "peri" fluorine atom. On the other hand, π–π interactions in aromatic compounds[21-24] are well known to skew the rotameric preferences of aryl amides. To shed light on the relative stabilities of the rotamers - and thereby possible H-bonding interactions - we turned to DFT calculations. At ωB97XD/6-311+G**, we located the cis and trans rotamers for each derivative (Figure **2**, see supporting information "SI" for details). In trans structures **1-4**, the NH hydrogen resides at a position maximizing the NH···F interaction, whereas it bends out of the plane of naphthalene ring in cis structures **1a-4a**, thus attenuating the interaction (Figure **2**). As it were, the desired rotamers were predicted to be more stable by at least 2.3 kcal/mol as we would ordinarily expect. Additionally, the amide NH···F distances in the series **1-4** are predicted to lie in the range of 1.84-1.86 Å (gas phase), smaller than the shortest distance of 1.93 Å observed crystallographically.[14]

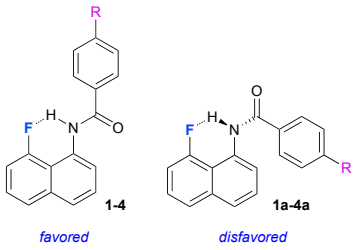

Figure 2. *Rotameric forms located by DFT calculations (ωB97XD/6-311+G**) with **1-4** favored over **1a-4a** by >2.7 kcal/mol.*

Curiously, replacing the fluorine with hydrogen attenuates the preference for the desired rotamer and no stability trend is observed when test molecules **5** were optimized at the same level of theory (Figure **3**, Table **S2**). In fact, the NH proton bends out of the plane of the naphthalene ring in both optimized rotamers (See SI). Similarly, no noticeable trend was observed when rotamers of 7-fluoro-1-aminonaphthalene derivatives were optimized (**6**, Figure **3**, Table **S3**). These calculations suggested to us that the relative stability of desired rotamers could be attributed in part to favorable NH···F interactions. Therefore, having a fluorine atom at that position may prove essential to the investigation as it locks the structure in the desired orientation.

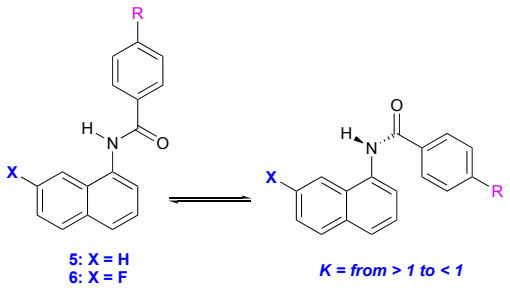

Figure 3. *Rotamers of **5** and **6** optimized for rotameric preferences with DFT calculations at ωB97XD/6-311+G**; R = NMe_2; OMe; H; NO_2.*

After DFT calculations pointed us in the right direction, we synthesized the desired molecules from commercially available 1,8-diaminonaphthalene **8**. Treatment of **8** with isoamyl nitrite followed by HF-pyridine resulted in the formation of 8-fluoro-1-aminonaphthalene **10**,[25] which was then acetylated with a series of substituted benzoyl chlorides to afford N-(8-fluoronahphthalen-1-yl)benzamide derivatives in 75-85% yields (Scheme **1**). The dimethylamino analogue **4** was synthesized by reduction/alkylation of p-NO_2 derivative **3** (Scheme **1**).

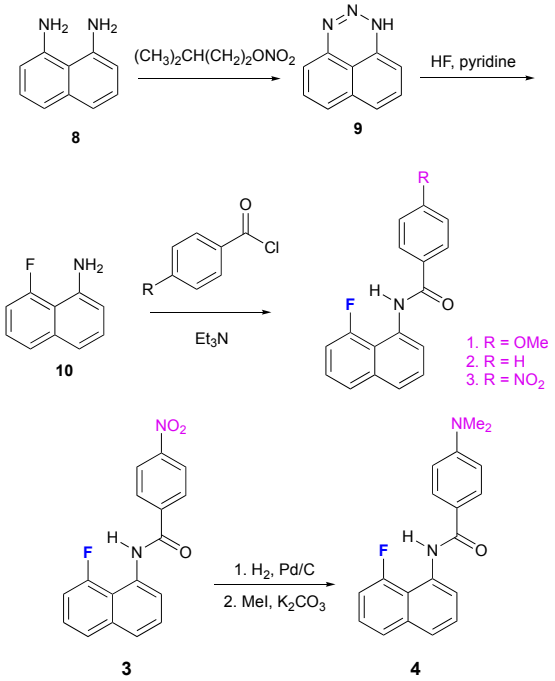

Scheme 1. *Synthesis of N-(8-fluoronahphthalen-1-yl) benzamide derivatives.*

The two rotamers can easily be distinguished based on the NH···F spin-spin coupling constants predicted by DFT calculations (B3LYP/6-311++G**). In *trans*-amide conformations, the calculated coupling constants lie between 24-27 Hz, whereas for the undesired rotamers as well as rotamers of **5** and **6** those numbers drop to 0-2 Hz. Experimentally, the ^{1}H NMR spectra of all derivatives show NH protons as apparent doublets (J_{H-F} = 20-21 Hz). On the other hand, the ^{19}F NMR spectra reveal complex multiplets (See SI). Both ^{1}H and ^{19}F NMR spectra indicate that the products of Scheme **1** are locked exclusively in the desired *trans* orientation. The ^{19}F NMR of all the derivatives also reveal consistent 16 Hz coupling constants corresponding to the interaction of the F nucleus with the ortho proton on the naphthalene ring system[16] (calcd 16.4 Hz, Figure **4**). Additionally, the coupling constants for the series are predicted to show a slight increase as the substituent on the benzene ring becomes more electron withdrawing (from 24.7 Hz for p-NMe_2 to 27 Hz for p-NO_2). However, this modest trend is not clearly discernable in the actual ^{19}F NMR data primarily due to the complex nature of the multiplets.

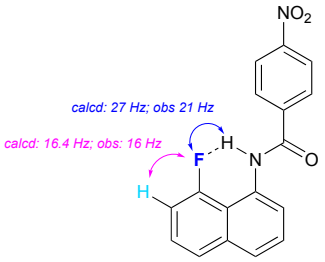

Figure 4. *Major coupling constants observed experimentally and predicted by B3LYP/6-311++G** (compound **3**).*

We then conducted an IR analysis of the NH···F interactions. It is generally accepted that the increasing strength of a classical hydrogen bond results in lengthening of the donor-H bond and an attendant shortening of the acceptor-H distance, inducing a red shift

in the IR-stretching frequency.[26-30] An initial DFT analysis (ωB97XD/6-311+G**) of the synthesized molecules predicts a similar trend for NH stretches in the IR as the nature of substituent becomes more electron withdrawing, a possible indication of increasing hydrogen bond strength (Table **1**).

Table 1. *Calculated (scaled) and experimentally observed NH stretching frequencies in **1** through **4**.*

NH stretch cm^{-1}	R = NMe_2	OMe	H	NO_2
predicted	*3517*	*3516*	*3503*	*3501*
experimental	*3486*	*3482*	*3477*	*3471*

The NH stretch in the experimentally observed IR spectra of the derivatives shows a continuous high energy shift as the aromatic ring becomes more electron deficient. The NH stretch of p-NO_2 derivative appears at 3470.5 cm^{-1}, which is ca. 16 cm^{-1} red shifted compared to the same stretch in the p-NMe_2 derivative, thus implying a significantly stronger H bond in the former case (Table **1** and Figure **5**). Although substituent effects have a relatively smaller effect on high energy shifts in the NH stretching frequency of benzamides, this fact does not necessarily imply a weak substituent effect on the hydrogen bond strength itself since the high energy shift in IR is considered only a semi-quantitative measure.[31]

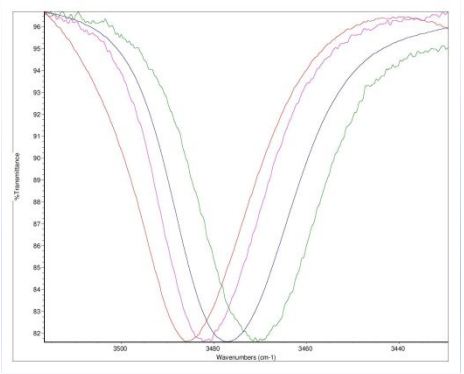

Figure 5: *Experimentally observed NH stretches in IR spectra; red (p-NMe_2); purple (p-OMe); blue (p-H); green (p-NO_2).*

X-ray crystallographic analysis gives additional insight into the influence of fluorine substitution on crystal packing. We recently reported the crystal structure of a substituted trityl fluoride that is significantly different than the corresponding trityl hydride, confirming the inability of fluorine to act as an "isostere" for hydrogen when it comes to directionality/ordering.[32] Single crystal X-ray analysis of the p-NO_2 derivative **3** reveals an interesting feature; the naphthalene rings are aligned face to face in a π–π interaction (Figure **6**), which is significantly different than the crystal structure of *N*-(naphthalen-1-yl)benzamide, wherein the phenyl ring engages in T-shaped π–π interactions with the naphthalene ring system.[33] This motif results in the formation of naphthalene-based sheets held by intermolecular hydrogen bonding between the amide N-H and a neighboring molecule's carbonyl oxygen at 2.12 Å. Moreover, the NH···F and N-H distances of 2.22 Å and 0.87 Å are observed in the crystal structure of p-NO_2 benzamide derivative (Figure **6**, See SI for details).

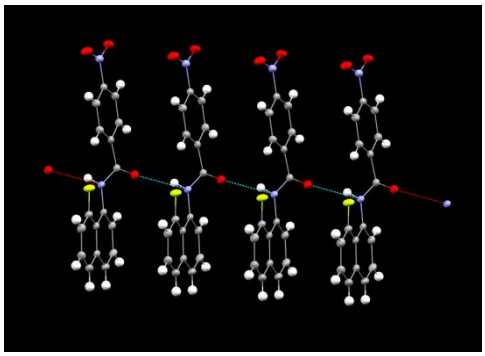

Figure 6. *X-ray crystal structure of p-NO_2 benzamide derivative (**3**) with extended hydrogen bonding network forming sheets of naphthalene rings.*

Finally, we imagined that an even larger high energy IR shift could be observed if the substituent is more electron withdrawing than p-NO_2Ph. A DFT analysis predicted that replacing the benzamide derivatives with trifluoroacetamide would show a significant red shift of an additional 39 cm^{-1} in NH stretching frequency compared to p-NO_2Ph derivative. In fact, when 8-fluoro-1-aminonaphthalene is acetylated with trifluoroacetic anhydride (Scheme **2**, 86%), the NH stretch of the product appears at 3443 cm^{-1}, red shifted by 28 cm^{-1} compared to the p-NO_2 derivative (Figure **7**). Additionally, its ^{19}F NMR spectrum shows a multiplet corresponding to aromatic fluorine with a spin-spin coupling constant of 19.1 Hz to the proximate N-H, even larger than that observed in **3**.

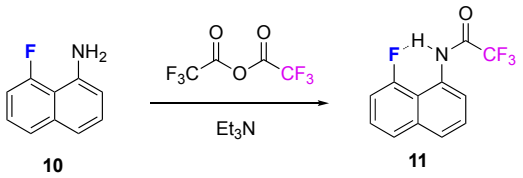

Scheme 2. *Synthesis of the trifluoroacetamide derivative **11**.*

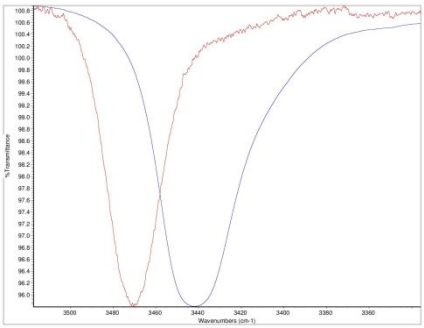

Figure 7. *Experimentally observed NH stretches in IR spectra; red (p-NO_2Ph) peak at 3470.5 cm^{-1}; blue (CF_3) peak at 3442.9 cm^{-1}.*

Single crystal X-ray analysis of the trifluoroacetamide derivative **11** also reveals an interesting structure. Similar to the benzamide derivatives, the crystal is characterized by sheets and bifurcated C-F···HN bonding with an amide carbonyl oxygen and fluorine on position 8 of the naphthalene ring (NH···F, 2.12 Å), (NH···O, 2.19 Å), (N-H···F_3C, 2.25 Å). Another interesting feature of trifluorobenzamide derivative's crystal structure is the close F···F distance (2.98 Å) between the neighboring molecules' CF_3 groups (Figure **8**).

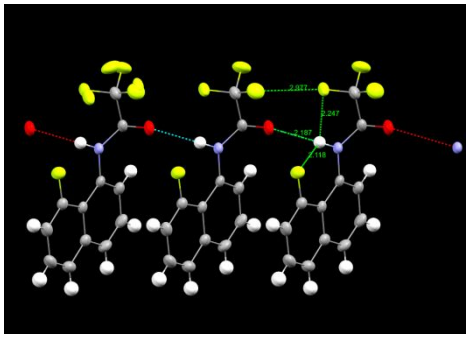

Figure 8. *X-ray crystal structure of trifluoroacetamide derivative* ***11*** *depicting an extended hydrogen bonding network forming sheets of naphthalene rings.*

The X-ray crystal structures of **3** and **11**, however, depict amide NH···F distances of 2.22 Å and 2.12 Å respectively, which are greater than the shortest NH···F distance found in the CCD and our predicted gas phase distances. This increased distance in the crystal structures can be attributed to intermolecular hydrogen bonding with neighboring molecule's carbonyl oxygen. In dilute solutions, however, we conclude that the intramolecular NH···F interaction dominates and the distance could be approximated to, or even smaller, than 1.93 Å. We optimized a few of the structures with the shortest NH···F distances reported in the CCD[34-37] at ωB97XD/6-311+G** and calculated spin-spin coupling constants for the NH···F interactions therein at B3LYP/6-311++G** (See SI for structures and computational details). DFT calculations predict an inverse correlation of the NH···F coupling constants and distances between the interacting nuclei (Figure **9**). The largest amide NH···F coupling constant reported in the literature is 17.1 Hz.[35] This is smaller than those observed in our molecules which are, both predicted and experimentally, more than 20 Hz, indicating the *possibility* of an amide NH···F distance shorter than those observed so far. The trend in Figure **9** predicts NH···F distances in the series of our benzamide derivatives to be approximately 1.90 Å in dilute solutions, in line with DFT geometry calculations. However, when it comes to crystal packing, the NH proton skews out of the plane of naphthalene ring as a result of competitive intermolecular NH···OC hydrogen bonding.

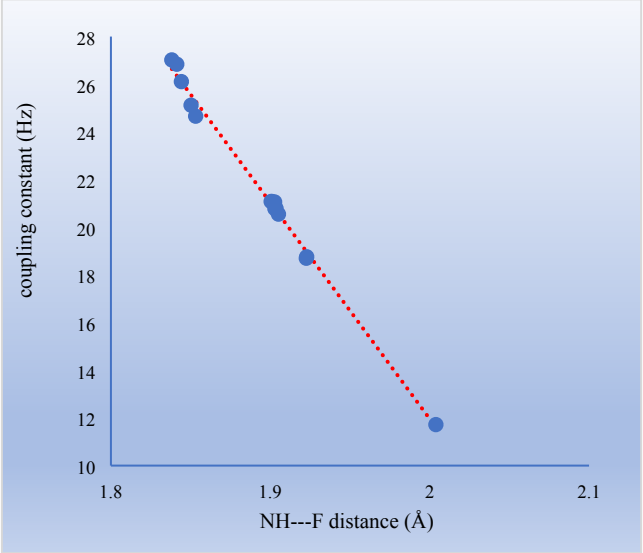

Figure 9: *Correlation between calculated NH···F distances and corresponding coupling constants calculated at B3LYP/6-311++G** using molecules* ***1-4*** *and* ***11-20****. See SI for details.*

Conclusion

In this note, we have synthesized a series of N-(8-fluoronaphthalen-1-yl)benzamide derivatives and established a correlation between the strength of NH···F hydrogen bonding interaction and substituents on the benzamide ring. Both ^{1}H and ^{19}F NMR spectra indicate the exclusive formation of the desired geometry, attributed to the favorable hydrogen bonding interactions, most notably through strong spin-spin coupling of H and F. Moreover, IR analysis of the series predicts a direct correlation between the electron withdrawing nature of substituent and the hydrogen bond strength. X-ray crystallographic analysis reveals the formation of sheets characterized by face-to-face π–π interactions between the naphthalene rings. We hope that these results provide additional insights into the increasingly important role of fluorine in hydrogen bonding interactions.

Experimental Section

^{1}H and ^{13}C spectra were acquired on a 400 MHz NMR in $CDCl_3$ at 25 °C while ^{19}F spectra were acquired on a 300 MHz NMR in $CDCl_3$. The ^{1}H, ^{13}C and ^{19}F chemical shifts are given in parts per million (δ) with respect to an internal tetramethylsilane (TMS, δ 0.00 ppm) standard. NMR data are reported in the following format: chemical shifts (multiplicity (s = singlet, d = doublet, t = triplet, q = quartet m = multiplet), coupling constants [Hz], integration). IR data were obtained using an FT-IR with a flat CaF_2 cell. HRMS data were obtained on a Thermo Scientific Q-Exactive Orbitrap mass spectrometer.

General protocol for synthesis of the N-(8-fluoronaphthalen-1-yl)benzamide derivatives: To a solution of **10** in 10 mL CH_2Cl_2, 1 equiv. of the appropriate benzoyl chloride derivative was added at room temperature. To the mixture, 0.1 mL Et_3N was added and the solution was stirred at room temperature for 2 h. The solvent was evaporated under reduced pressure and the desired product was purified with MPLC using hexanes and ethyl acetate as eluents.

N-(8-fluoronaphthalen-1-yl)-4-methoxybenzamide (compound ***1****).* Compound **1** was synthesized following the general protocol for benzamide derivative synthesis and isolated as colorless crystalline solid (135 mg, 75% isolated yield). ^{1}H NMR ($CDCl_3$) δ 9.6 (d, J = 20.6 Hz, 1H), 8.76 (d, J = 7.7 Hz, 1H), 7.94 (d, J = 8.7 Hz, 1H), 7.5–7.66 (m, 3H), 7.3–7.4 (m, 1H), 7.1–7.2 (m, 1H), 7.01 (d, J = 8.7Hz, 1H), 3.88 (s, 3H); ^{13}C NMR {^{1}H} ($CDCl_3$) δ 165, 164.97, 165.5, 160.3, 157.9, 136.6, 136.5, 132.93, 132.89, 128.8, 127.4, 127.30, 127.29, 125.56, 125.46, 125.41, 125.38, 123.70, 123.67, 118.32, 118.30, 115.05, 114.97, 114.1, 111.3, 111.1, 55.5; ^{19}F NMR ($CDCl_3$) δ –117 (m, 1F); ^{19}F NMR {^{1}H} ($CDCl_3$) δ –117 (s, 1F); IR 3482, 1675, 1606, 1537, 1495, 1432, 1341 (cm^{-1}, CaF_2, CH_2Cl_2); FTMS (ESI) m/z: [M + H]+ Calcd for $C_{18}H_{15}FNO_2$+ 296.1081; Found 296.1076.

N-(8-fluoronaphthalen-1-yl)benzamide (compound ***2****).* Compound **2** was synthesized following the general protocol for benzamide derivative synthesis and isolated as a light pink solid (145 mg, 80% isolated yield). ^{1}H NMR ($CDCl_3$) δ 9.69 (d, J = 20.8 Hz, 1H), 8.73 (d, J = 7.86 Hz, 1H), 8.38 (m, 2H), 8.13 (m, 2H), 7.7 (m, 2H), 7.5–7.6 (t, J = 8 Hz, 1H), 7.4–7.47 (m, 1H), 7.19–7.25 (m, 1H); ^{13}C NMR {^{1}H} ($CDCl_3$) δ 163.3, 160.1, 157.7, 149.8, 140.7, 136.51,

136.48, 131.95, 131.91, 128.1, 127.23, 127.21, 125.93, 125.82, 125.62, 125.59, 124.81, 124.79, 124.2, 118.91, 118.89, 150.07, 149.99, 111.7, 111.5; ^{19}F NMR ($CDCl_3$) δ –116.96 (m, 1F); ^{19}F NMR {^{1}H} ($CDCl_3$) δ –116.96 (s, 1F); IR 3477, 1681, 1541, 1487, 1432, 1342 (cm^{-1}, CaF_2, CH_2Cl_2); FTMS (ESI) m/z: [M + H]+ Calcd for $C_{17}H_{13}FNO$+ 266.0976; Found 266.0970.

N-(8-fluoronaphthalen-1-yl)-4-nitrobenzamide (compound 3). Compound **3** was synthesized following the general protocol for benzamide derivative synthesis and isolated as a yellow solid (162 mg, 85% isolated yield). ^{1}H NMR ($CDCl_3$) δ 9.7 (d, J = 21 Hz, 1H), 8.79 (m, 1H), 7.98 (m, 1H), 7.5–7.68 (m, 6H), 7.34–7.42 (m, 1H), 7.15–7.23 (m, 1H); ^{13}C NMR {^{1}H} ($CDCl_3$) δ 165.45, 165.43, 160.3, 157.8, 136.55, 136.51, 135.2, 132.72, 132.68, 131.9, 128.9, 127.30, 127.29, 126.9, 125.6, 125.5, 125.44, 125.40, 123.98, 123.95, 118.49, 118.47, 115.1, 115, 111.4, 111.2; ^{19}F NMR ($CDCl_3$) δ –117 (m, 1F); ^{19}F NMR {^{1}H} ($CDCl_3$) δ –117 (s, 1F); IR 3470, 1688, 1606, 1540, 1531, 1503, 1487, 1347 (cm^{-1}, CaF_2, CH_2Cl_2); FTMS (ESI) m/z: [M + H]+ Calcd for $C_{17}H_{12}FN_2O_3$+ 311.0826; Found 311.0819.

Synthesis of 4-(dimethylamino)-*N*-(8-fluoronaphthalen-1-yl)benzamide (compound 4): Compound **3** (100 mg, 0.32 mmol) was dissolved in 30 mL EtOH:THF (2:1) and Pd/C was added to the solution. The mixture was purged with H_2 gas until TLC indicated complete consumption of **3** and the mixture was purged with excess H_2 gas for another 30 min. Pd/C was then filtered through celite and the cake was washed with 15 mL THF. The solvent was evaporated under reduced pressure and the ^{1}H NMR of mixture indicated complete conversion of NO_2 to NH_2. The intermediate p-NH_2 derivative was utilized without further purification. It was dissolved in 20 mL EtOH, 200 mg (1.45 mmol) of K_2CO_3 and 0.1 mL (1.6 mmol) MeI were added to the mixture and the solution was refluxed overnight. The reaction mixture was filtered over Celite, washed with 10 mL EtOH and filtrate was evaporated under reduced pressure. The dimethylated product was isolated by MPLC using hexanes and ethyl acetate as eluent as a light pink solid (35 mg, 35% isolated yield). ^{1}H NMR ($CDCl_3$) δ 9.63 (d, J = 21.1 Hz, 1H), 8.82 (m, 1H), 7.88 (m, 2H), 7.5–7.67 (m, 3H), 7.3–7.41 (m, 1H), 7.12–7.22 (m, 1H), 6.76 (m, 2H), 3.06 (s, 6H); ^{13}C NMR {^{1}H} ($CDCl_3$) δ 165.49, 165.47, 160.5, 158.1, 152.7, 136.62, 136.58, 128.5, 127.42, 127.40, 125.42, 125.38, 125.35, 125.32, 123.17, 123.14, 121.8, 117.97, 117.95, 114.98, 114.90, 111.3, 111.2, 110.9, 40.1; ^{19}F NMR ($CDCl_3$) δ –116.29 (m, 1F); ^{19}F NMR {^{1}H} ($CDCl_3$) δ –116.29 (s, 1F); IR 3486, 1669, 1607, 1541, 1526, 1501 (cm^{-1}, CaF_2, CH_2Cl_2); FTMS (ESI) m/z: [M + H]+ Calcd for $C_{19}H_{18}FN_2O$+ 309.1398; Found 309.1392.

Synthesis of 2,2,2-trifluoro-*N*-(8-fluoronaphthalen-1-yl)acetamide (compound 11): To a solution of **10** (110 mg, 0.68 mmol) in 10 mL DCM was added 0.1 mL (0.7 mmol) of trifluoroacetic anhydride and 0.1 mL Et_3N. After stirring at room temperature for 2 h, the solvent was evaporated under reduced pressure and the product was purified on MPLC using hexanes and ethyl acetate as eluents as a white solid (150 mg, 86% isolated yield). ^{1}H NMR ($CDCl_3$) δ 9.7 (d, J = 19.9 Hz, 1H), 8.52 (m, 1H), 7.6–7.8 (m, 2H), 7.5–7.59 (m, 1H), 7.4–7.49 (m, 1H), 7.15–7.3 (m, 1H); ^{13}C NMR {^{1}H} ($CDCl_3$) δ 159.7, 157.3, 155, 154.6, 136.31, 136.28, 129.74, 129.70, 126.96, 126.94, 126.3, 126.2, 125.97, 125.94, 125.50, 125.46, 120.1, 119.36, 119.34, 117.3, 115.0, 114.9, 114.4, 112.1, 111.9; ^{19}F NMR ($CDCl_3$) δ –117.9 (m, 1F), –76.19 (s, 3F); IR 3443, 1737, 1638, 1555, 1507, 1443, 1382 (cm^{-1}, CaF_2, CH_2Cl_2); FTMS (ESI) m/z: [M + H]+ Calcd for $C_{12}H_8F_4NO$+ 258.0536; Found 258.0530.

ASSOCIATED CONTENT

Supporting Information

NMR spectra, crystal structure data, and computational information are included in the Supporting Information.

Crystal Structure of Compound **3** (CCDC 1987532)

Crystal Structure of Compound **11** (CCDC 1987533)

AUTHOR INFORMATION

Corresponding Author

* Email: lectka@jhu.edu

ORCID

Muhammad Kazim: 0000-0003-2020-8952

Notes

The authors declare no competing financial interest.

ACKNOWLEDGMENT

T.L. thanks the National Science Foundation (Grant CHE 1800510) for financial support. Mass spectral data were obtained at University of Delaware's mass spectrometry center.

REFERENCES

1 Vishnumurthy, K.; Row, T. N. G.; Venkatesan; K. Fluorine in Crystal Engineering: Photodimerization of (1*E*,3*E*)-1-phenyl-4-pentafluorophenylbuta-1,3-dienes in the Crystalline State. Photoch. *PhotoBio. Sci.* **2002**, *6*, 427-430.

2 Kawahara, S.; Tsuzuki, S.; Uchimaru, T. Theoretical Study of the C-F/π Interaction: Attractive Interaction Between Fluorinated Alkane and an Electron-Deficient π-System. *J. Phys. Chem. A* **2004**, *108*, 6744-6749.

3 Jackel, C.; Koksch, B. Fluorine in Peptide Design and Protein Engineering. *Eur. J. Org. Chem.* **2005**, *21*, 4482-4503.

4 Riley, K. E.; Merz, K. M. Effects of Fluorine Substitution on the Edge-to-Face Interaction of Benzene Dimer. *J. Phys. Chem. B* **2005**, *109*, 17752-17756.

5 Chopra, D.; Nagarajan, K.; Row, T. N. G. Analysis of Weak Interactions Involving Organic Fluorine: Insights From Packing Features in Substituted 4-Keto-tetrahydroindoles. *J. Mol. Struct.* **2008**, *888*, 70-83.

6 Zhou, P.; Zou, J.; Tian, F.; Shang, Z. Fluorine Bonding – How Does It Work In Protein – Ligand Interactions? *J. Chem. Inf. Model.* **2009**, *49*, 2344-2355.

7 Struble, M. D.; Guan, L.; Siegler, M. A.; Lectka, T. A C–F Bond Directed Diels–Alder Reaction. *J. Org. Chem.* **2016**, *81*, 8087-8090.

8 Holl, M. G.; Struble, M. D.; Singal, P.; Siegler, M. A.; Lectka, T. Positioning a Carbon-Fluorine Bond Over the π Cloud of an Aromatic Ring: A Different Type of Arene Activation. *Angew. Chem. Int. Ed.* **2016**, *55*, 8266-8269.

9 Struble, M. D.; Kelly, C.; Siegler, M. A.; Lectka, T. Search for a Strong, Virtually "No Shift" Hydrogen Bond: A Cage Molecule with an Exceptional OH---F Interaction. *Angew. Chem. Int. Ed.* **2014**, *53*, 8924-8928.

10 Holl, M. G.; Pitts, C. R.; Lectka, T. Quest for a Symmetric [C–F–C]$^+$ Fluoronium Ion in Solution: A Winding Path to Ultimate Success. *Acc. Chem. Res.* **2020**, *53*, 265-275.

11 Pitts, C. R.; Siegler, M. A.; Lectka, T. Intermolecular Aliphatic C–F---H–C Interaction in the Presence of "Stronger" Hydrogen Bond Acceptors: Crystallographic, Computational, and IR Studies. *J. Org. Chem.* **2017**, *82*, 3996-4000.

12 Holl, M. G.; Struble, M. D.; Siegler, M. A.; Lectka, T. The Close Interaction of a C–F Bond with a Carbonyl π-System: Attractive, Repulsive, or Both? *J. Fluorine Chem.* **2016**, *188*, 126-130.

13 Holl, M. G.; Pitts, C. R.; Lectka, T. Fluorine in a C–F Bond as the Key to Cage Formation. *Angew. Chem. Int. Ed.* **2018**, *57*, 2758-2766.

14 Zhu, W.; Yang, W.; Zhou, W.; Liu, H.; Wei, S.; Fan, J. A. New Crystal Structure and Fluorescence Property of N-2-Fluorobenzoyl-N'-4-tolylthiourea. *J. Mol. Struct.* **2011**, *1004*, 74-81.

15 Cox, C.; Wack, H.; Lectka, T. Strong Hydrogen Bonding to the Amide Nitrogen Atom in an "Amide Proton Sponge": Consequences for Structure and Reactivity. *Angew. Chem. Int. Ed.* **1999**, *38*, 798-800.

16 Scerba, M. T.; Leavitt, C. M.; Diener, M. E.; DeBlase, A. F.; Guasco, T. L.; Siegler, M. A.; Bair, N.; Johnson, M. A.; Lectka, T. NH$^+$–F Hydrogen Bonding in a Fluorinated "Proton Sponge" Derivative: Integration of Solution, Solid-State, Gas-Phase, and Computational Studies. *J. Org. Chem.* **2011**, *76*, 7975-7984.

17 Alder, R. W.; Bowmann, P. S.; Steele, W. R. S.; Winterman, D. R. The Remarkable Basicity of 1,8-Bis(dimethylamino)naphthalene. *Chem. Commun.* **1968**, *13*, 723-724.

18 Staab, H. A.; Saupe, T. "Proton Sponges" and the Geometry of Hydrogen Bonds: Aromatic Nitrogen Bases with Exceptional Basicities. *Angew. Chem. Int. Ed.* **1988**, *27*, 865-879.

19 Alder, R. W. Strain Effects on Amine Basicities. *Chem. Rev.* **1989**, *89*, 1215-1223.

20 Hibbert, F.; Emsley, J. Hydrogen Bonding and Chemical Reactivity. *Adv. Phys. Org. Chem.* **1990**, *26*, 255-379.

21 Hunter, C. A.; Sanders, J. K. M. The Nature of π–π Interactions. *J. Am. Chem. Soc.* **1990**, *112*, 5525-5534.

22 Hunter, C. A.; Singh, J.; Thornton, J. M. π–π Interactions: The Geometry and Energetics of Phenylalanine-Phenylalanine Interactions in Proteins. *J. Mol. Biol.* **1991**, *218*, 837-846.

23 Martinez, C. R.; Iverson, B. L. Rethinking the Term "pi-stacking." *Chem. Sci.* **2012**, *3*, 2191-2201.

24 Sony, S. M. M.; Ponnuswamy, M. N. Nature of π Interactions in Nitrogen-Containing Heterocyclic Systems: A Structural Database Analysis. *Cryst. Growth Des.* **2006**, *6*, 736-742.

25 Zhu, Z.; Colbry, N. L.; Lovdahl, M.; Mennen, K. E.; Acciacca, A.; Beylin, V. G.; Clark, J. D.; Belmont, D. T. Practical Alternative Synthesis of 1-(8-Fluoro-naphthalen-1-yl-)piperazine. *Org. Prep. Process Res. Dev.* **2007**, *11*, 907–909.

26 Arunan, E.; Desiraju, G. R.; Klein, R. A.; Sadlej, J.; Scheiner, S.; Alkorta, I.; Clary, D. C.; Crabtree, R. H.; Dannenberg, J. J.; Hobza, P.; Kjaergaard, H. G.; Legon, A. C.; Mennucci, B.; Nesbitt, D. J. Definition of the Hydrogen Bond (IUPAC Recommendations 2011). *Pure Appl. Chem.* **2011**, *83*, 1637-1641.

27 Joseph, J.; Jemmis, E. D. Red-, Blue- or No-Shift in Hydrogen Bonds: A Unified Explanation. *J. Am. Chem. Soc.* **2007**, *129*, 4620-4632.

28 Duarte, L. J.; Silva, A. F.; Richter, W. E.; Bruns, R. E. Infrared Intensification and Hydrogen Bond Stabilization: Beyond Point Charges. *J. Phys. Chem. A* **2019**, *123*, 6482-6490.

29 Mao, Y.; Gordon, M. H. Probing Blue-Shifting Hydrogen Bonds with Adiabatic Energy Decomposition Analysis. *J. Phys. Chem. Lett.* **2019**, *10*, 3899-3905.

30 Wang, C.; Mo, Y. Classical Electrostatic Interaction is the Origin for Blue-Shifting Halogen Bonds. *Inorg. Chem.* **2019**, *58*, 8577-8586.

31 Rosenberg, M.; Loewenschuss, A.; Marcus, Y. An Empirical Correlation Between Stretching Vibration Redshift and Hydrogen Bond Length. *Phys. Chem. Chem. Phys.* **2000**, *2*, 2699-2702.

32 York, G. D.; Siegler, M. A.; Patel, D. D.; Lectka, T. Synthesis and X-Ray Crystallography of a Substituted Trityl Fluoride: Ordering Power of a C–F Bond. *J. Fluor. Chem.* **2019**, *228*, 109377.

33 Zhu, R.; Ren, Y.; Li, W. *N*-(Napthalen-1-yl)benzamide. *Acta Cryst.* **2011**, E**67**, o3204. DOI: 10.1107/S1600536811045946.

34 Zhao, X.; Wang, X. Z.; Jiang, X. K.; Chen, Y. Q.; Li, Z. T.; Chen, G. J. Hydrazide-Based Quadruply Hydrogen-Bonded Heterodimers. Structure, Assembling Selectivity, and Supramolecular Substitution. *J. Am. Chem. Soc.* **2003**, *125*, 15128-15139.

35 Li, C.; Ren, S. F.; Hou, J. L.; Yi, H. P.; Zhu, S. Z.; Jiang, X. K.; Li, Z. T. F---H–N Hydrogen Bonding Driven Foldamers: Efficient Receptors for Dialkylammonium Ions. *Angew. Chem. Int. Ed.* **2005**, *44*, 5725-5729.

36 Zhu, K. Y.; Wu, J.; Li, C.; Zhu, J.; Hou, J. L.; Li, C. Z.; Jiang, X. K.; Li, Z. T. F---H–N and MeO---H–N Hydrogen Bonding in the Solid States of Aromatic Amides and Hydrazides: A Comparison Study. *Crys. Growth Des.* **2007**, *7*, 1490-1496.

37 Bhandary, S.; Gonde, S.; Chopra, D. Dissecting the Conformational and Interaction Topological Landscape of *N*-ethynylphenylbenzamide by the Device of Polymorphic Diversity. *Cryst. Growth Des.* **2019**, *19*, 1072-1085.
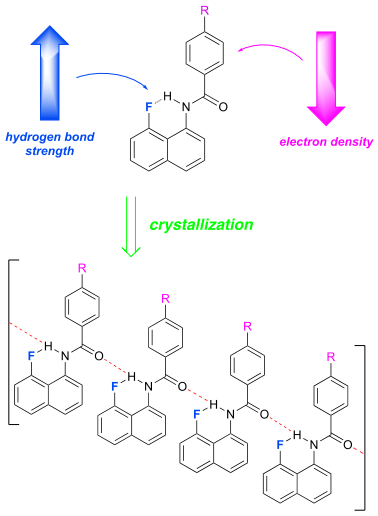
Insert Table of Contents artwork here